Special Feature: Recent Research Developments on Periodic Mesoporous Organosilicas

Research Report

Catalysis of Metal Complexes Immobilized on Periodic Mesoporous Organosilicas

Yoshifumi Maegawa

▮**ABSTRACT**▮ The immobilization of homogeneous transition-metal complexes onto solid supports is an important catalyst technology in industrial chemical processes because heterogeneous catalysts have crucial advantages such as easy handling, separation, and reusability. However, conventional immobilization approaches suffer from loss of the metal coordination structure of the active centers, which decreases the catalytic activity and selectivity of the original homogeneous metal complex catalyst. Recently, we synthesized a crystal-like bipyridine-bridged periodic mesoporous organosilica (BPy-PMO) as a new class of solid chelating ligand to construct a well-defined metal coordination structure on the support surface. This report describes the synthesis of BPy-PMO and recent advances in the development of highly active heterogeneous metal complex catalysts immobilized on BPy-PMO. BPy-PMO demonstrated great potential for the heterogenization of homogeneous metal complex catalysts. We developed highly active heterogeneous metal complex catalysts for direct C-H borylation of arenes and heteroarenes with bis(pinacolate)diboron or pinacolborane, and epoxidation of olefins with *tert*-butyl hydroperoxide without loss of the original performance of the homogeneous metal complex catalysts.

▮**KEYWORDS**▮ Periodic Mesoporous Organosilica, Bipyridine, Solid Chelating Ligand, Transition-metal Complex, Homogeneous Catalyst, Heterogeneous Catalyst, Immobilization, Local Structure

1. Introduction

Transition-metal complex catalysts are widely used for the industrial production of pharmaceuticals, agrichemicals, and functional materials.[1] From the point of view of green chemistry, heterogenization of homogeneous metal complex catalysts has attracted much attention due to the easy catalyst separation, efficient recycling, and minimal metal leaching into the final products. Although numerous immobilization techniques of homogeneous catalysts have been studied, their catalytic activity and selectivity usually decrease after immobilization onto solid supports (**Fig. 1**(a)). This behavior is mainly caused by microenvironmental changes around the metal center and the increased diffusion limitation after heterogenization.[2] Development of an immobilization approach that preserves the well-defined metal coordination structure at the molecular level is required to maintain the inherent performance of homogeneous catalysts.

Periodic mesoporous organosilicas (PMOs), synthesized from organic-bridged alkoxysilane precursors $[(R'O)_3Si-R-Si(OR')_3, R = $ organic group, $R' = $ Me, Et, *i*-Pr] by surfactant-templated supramolecular assembly, are a new class of ordered mesoporous materials in which the organic groups are densely and covalently embedded within the silica framework.[3-5] We recently designed and synthesized a series of crystal-like PMOs bridged with chelating organic groups such as 2,5-divinylpyridine,[6] 2-phenylpyridine,[7] and 2,2'-bipyridine (BPy).[8,9] The pore surface of BPy-PMO is an ideal platform to construct a highly active heterogeneous metal complex catalyst with a well-defined metal coordination structure (Fig. 1(b)).[8] In this report, we describe the synthesis of BPy-PMO and recent advances in the development of metal complex catalysts immobilized on BPy-PMO and their unique catalytic performances.

2. BPy-PMO and Metal Complex Formation

### 2. 1 Synthesis and Structures of BPy-PMO

In 2014, we synthesized crystal-like BPy-PMO containing 2,2'-bipyridine within the pore wall

starting from 5,5'-bis(triisopropoxysilyl)-2,2'-bipyridine (**1**) as an organosilane precursor in the presence of a cationic surfactant template (**Fig. 2**(a)).[8] A well-ordered mesostructure was formed without the addition of other alkoxysilanes such as tetraethyl orthosilicate (TEOS). After extraction of the surfactant template using acidic ethanol solution, a well-ordered mesoporous structure was obtained. The X-ray diffraction (XRD) pattern of BPy-PMO showed characteristic diffraction peaks at 2θ = 1.96°, 3.40°, and 3.84° (d = 4.50, 2.60, 2.30 nm) corresponding to a two-dimensional (2D) hexagonal lattice of a well-ordered mesoporous structure. In addition, three peaks at a medium scattering angle of 5-35° corresponded to a crystal-like pore wall structure embedded with bipyridine groups. The nitrogen (N_2) adsorption/desorption isotherms of BPy-PMO were identified as type-IV, indicating the formation of a well-ordered mesoporous structure. Brunauer-Emmett-Teller surface area (S_{BET}), density functional theory pore diameter (d_{DFT}), and t-plot pore volume (V_{t-plot}) values of BPy-PMO were 739 m^2 g^{-1}, 3.8 nm, and 0.41 cm^3 g^{-1}, respectively. Figure 2(b-e) shows the scanning and transmission electron microscopy (SEM and TEM) images of BPy-PMO powder. The SEM image showed the aggregation of spherical particles with diameters of 200-500 nm (Fig. 2(b)). The TEM images clearly showed: i) one-dimensional channels going through the particles (Fig. 2(c)), ii) a 2D hexagonal arrangement of uniform pores (Fig. 2(d)), and iii) many lattice fringes corresponding to a lamellar structure of the bipyridine-silica units in the direction perpendicular to the pore channels (Fig. 2(e)). Figure 2(f) shows a structural image of BPy-PMO derived from molecular mechanics simulations. The bipyridine groups are densely packed and exposed on the pore surface. The distance between neighboring bipyridine ligands was estimated to be approximately 4.4 Å, slightly longer than the typical π-π stacking distance (3.5 Å) of aromatic rings. Bipyridine ligands would have a high degree of freedom to rotate about the Si-C axis in the framework. The bipyridine ligands in BPy-PMO have the ability to coordinate with a variety of metal ions.

## 2. 2 Immobilization of Metal Complexes on BPy-PMO

A well-defined metal complex can be directly formed on the pore surface of BPy-PMO. The metal complex formation is achieved by simply mixing BPy-PMO powder in a solution containing the metal complex precursor according to the procedure for homogeneous bipyridine-based metal complexes (**Fig. 3**(a)). For example, metalation between BPy-PMO and $Ru(bpy)_2Cl_2 \cdot 2H_2O$ in ethanol solution at 90°C afforded $Ru(bpy)_2(BPy\text{-}PMO)^{2+}$, which is a useful photosensitizer for photocatalytic reactions.[8] A variety of homogeneous bipyridine-based metal complexes including Ru,[8,10] Re,[8] Ir,[8,11,12] Pd,[8] Pt,[13,14] Rh,[15] Au,[16] Mn,[17] Mo,[18] and Cu[19] have been successfully immobilized onto the pore surface of BPy-PMO (Fig. 3(b)).
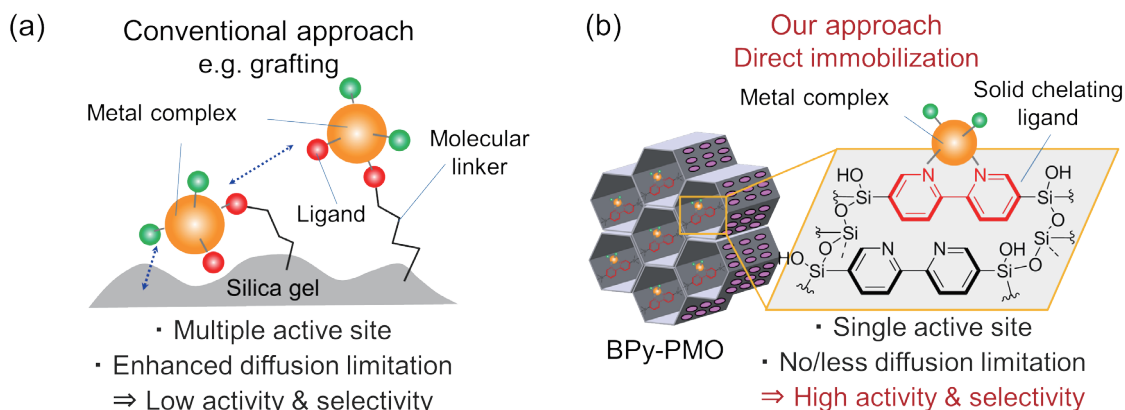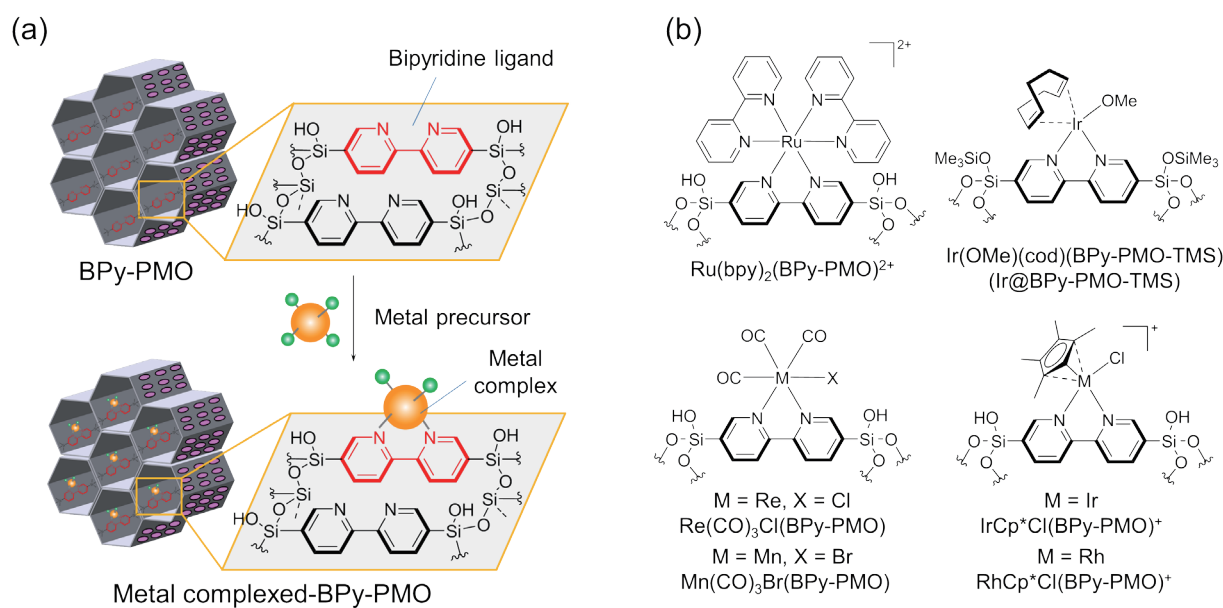

Fig. 1   Schematic illustration of immobilization of metal complex catalysts onto solid supports: (a) conventional approach (grafting method) and (b) our approach using BPy-PMO as a solid chelating ligand.

The loading amount of the metal complex on BPy-PMO can be controlled by changing the concentration of the metal precursor solution and the reaction conditions employed. The immobilization efficiency is largely dependent on the bulkiness and/or reactivity of the metal precursors against the
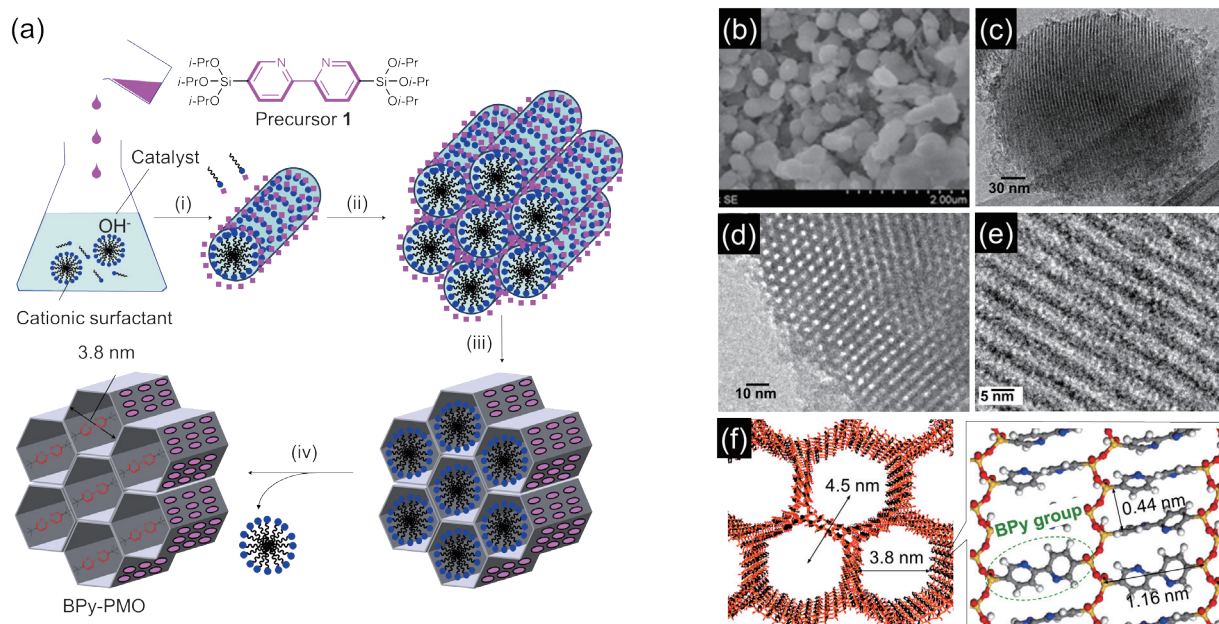
Fig. 2   (a) Schematic illustration of synthesis of BPy-PMO from bipyridine-bridged alkoxysilane precursor **1** by surfactant-templated supramolecular assembly: (i) hydrolysis of precursor, (ii) self-assembly, (iii) polycondensation, and (iv) removal of surfactant by solvent extraction, (b) SEM and (c)-(e) TEM images and (f) structural model of BPy-PMO. Silicon, yellow; oxygen, red; carbon, gray; nitrogen, blue; hydrogen, white.

Fig. 3   (a) Schematic illustration of direct metal complex formation of the pore surface of BPy-PMO. (b) Chemical structures of representative metal complexes immobilized on BPy-PMO or BPy-PMO-TMS as a solid chelating ligand.

embedded bipyridine ligand. Although the physical parameters such as surface area, pore volume and pore size are decreased slightly after immobilization of the metal complex, the obtained metal complexed-BPy-PMOs still have ordered mesoporous structures and molecular scale periodicity in the frameworks. The end-capping of silanol groups on the pore surface by trimethylsilyl reagents is an effective post-treatment to inhibit undesired metal complex formation between the surface silanol group and metal precursor. The passivation of silanol groups also improves the structural stability of the pore framework during the metal complex formation and the catalytic reaction.

2. 3　Characterization of Metal Complexed-BPy-PMO

Characterization of metal complexed-BPy-PMO can be carried out by various physicochemical analyses. Solid-state NMR spectroscopy is one of the most effective techniques for molecular-level investigation of chemical components in the organosilica framework including metal complex moieties. UV-vis diffuse reflectance and photoluminescence spectroscopies are useful techniques for characterization of the optical and electronic properties of immobilized metal complexes. Infrared (IR) and Raman spectroscopies are used to identify molecular structures and study chemical bonding and intramolecular interactions. X-ray photoelectron spectroscopy (XPS) is a surface-sensitive quantitative spectroscopic technique that measures the elemental composition and chemical and electronic states of the metal complex that exist on the pore surface. X-ray absorption fine structure (XAFS) analysis is a powerful tool to elucidate the local structure of immobilized metal complexes. X-ray absorption near edge structure (XANES) is an extremely useful way to determine the valence and coordination environment of metal centers. Extended X-ray absorption fine structure (EXAFS) gives useful information to determine the bond distance and coordination number of the metal center. The combination of these physicochemical analyses reveals that BPy-PMO can directly immobilize a well-defined metal complex at the molecular level that has an almost identical local structure as the corresponding homogeneous metal complex catalyst.

3. Heterogeneous Catalysis of BPy-PMO-based Metal Complexes

A well-defined metal complex catalyst immobilized on BPy-PMO has potential for high catalytic performance. The large pore size of BPy-PMO allows the smooth diffusion of reactant and product molecules in the mesochannels. The thermal stability and robust pore wall structure enable easy recovery and recycle use. We have thus far succeeded in immobilization of various metal complexes on BPy-PMO and demonstrated utilities of BPy-PMO-based metal complex catalysts for organic transformations and photocatalytic reactions. In this section, catalysis of BPy-PMO-based metal complexes for direct C-H borylation of arenes and heteroarenes, and epoxidation of olefins is described.

3. 1　Direct C-H Borylation of Arenes and Heteroarenes

Transition-metal catalyzed direct C-H borylation of arenes and heteroarenes is one of the most useful and straightforward synthetic strategies for aryl- and heteroarylboronate esters[20] which are useful intermediates for various organic transformations.[21] In particular, the Ir-bipyridine complex reported by the Ishiyama, Miyaura, and Hartwig groups is a reliable homogeneous catalyst and exhibits high catalytic activity and boron efficiency.[22]

We synthesized an iridium(methoxy)(cod)-bipyridine complex (cod: 1,5-cyclooctadiene) on the pore surface of trimethylsilylated BPy-PMO (denoted as BPy-PMO-TMS). The Ir complex was successfully synthesized by reacting BPy-PMO-TMS powder and [Ir(OMe)(cod)]$_2$ in benzene or hexane solution.[8,11] Structural analyses of the obtained Ir(OMe)(cod)(BPy-PMO-TMS) (denoted as Ir@BPy-PMO-TMS, Fig. 3(b)) by XRD and N$_2$ adsorption/desorption isotherm measurements revealed the preservation of a well-ordered mesoporous structure even after immobilization of the Ir complex. The local structure of the Ir center in Ir@BPy-PMO-TMS was almost identical to the corresponding homogeneous complex (Ir(OMe)(cod)(bpy)) as suggested by characteristic spectral data of XAFS and XPS measurements.

The catalytic activity of Ir@BPy-PMO-TMS for direct C-H borylation of arenes was examined by using bis(pinacolato)diboron (B$_2$pin$_2$, pin = O$_2$C$_2$Me$_4$) as a boron reagent under neat conditions (**Fig. 4**(a)).

The reaction between benzene and B_2pin_2 proceeded at 80°C to give phenylboronate ester (**2a**) in 94% yield after 4 h. The catalytic activity was greater than that of a homogeneous catalyst (Ir(OMe)(cod)(bpy), 80% yield) and heterogeneous catalysts that immobilized Ir-bipyridine complexes onto silica gel (Ir@BPy-Silica-TMS, 33% yield), mesoporous silica (Ir@BPy-FSM-TMS, 63% yield), and polystyrene (Ir@PS-BPy, no catalysis). From the reaction kinetic curves of these catalysts, Ir@BPy-PMO-TMS showed almost a constant reaction rate until the completion of the reaction, whereas other catalysts gradually decreased the reaction rate (Fig. 4(b)). In the case of the homogeneous catalyst, aggregation of the metal complex was observed after the reaction. This indicates decomposition of the homogeneous catalyst during the reaction. In cases of graft-type heterogeneous catalysts, the microenvironmental change of the local structure of the Ir-bipyridine complex would be induced by undesired interactions between the metal center and solid support and/or neighboring metal species due to the presence of flexible molecular linkers, which results in low catalysis. These results indicate that BPy-PMO is a useful solid chelating ligand for preparation of a well-isolated Ir-bipyridine complex and suppression of undesired interactions and aggregation of the active center during the reaction. Since the Ir-bipyridine complex was embedded in the covalent bonding

framework of Ir@BPy-PMO-TMS, no leaching of Ir species was observed in the filtered reaction solution even under heating conditions. The recovered Ir@BPy-PMO-TMS showed good reusability for at least three times, whereas other catalysts could not be used repeatedly.

The catalytic activity of Ir@BPy-PMO-TMS was further improved by using pinacolborane (HBpin) as the boron reagent. The benchmark reaction between benzene and HBpin under neat conditions gave a high turnover frequency (TOF) of 113 h^{-1}, which is 1.7 times greater than the reaction system using B_2pin_2 as a boron reagent. This means that HBpin is a preferable boron reagent for in-situ formation of an Ir-boryl complex on the pore surface as an active intermediate. The ease of formation of the active intermediate was also observed in diluted conditions with cyclohexane as a solvent. The reaction system using HBpin allowed reaction promotion even under dilute conditions and gave the product in 86% yield. In contrast, the reaction system using B_2pin_2 afforded only 4% yield under the same reaction conditions.

Ir@BPy-PMO-TMS also showed high catalytic activity for direct C-H borylation of substituted benzenes (**Table 1**). In the cases of electron-deficient benzenes containing CO_2Me and CF_3 groups, the reaction gave the corresponding arylboronate esters **2b-c** in high yields of 86-91% (Table 1, entries 1-2).
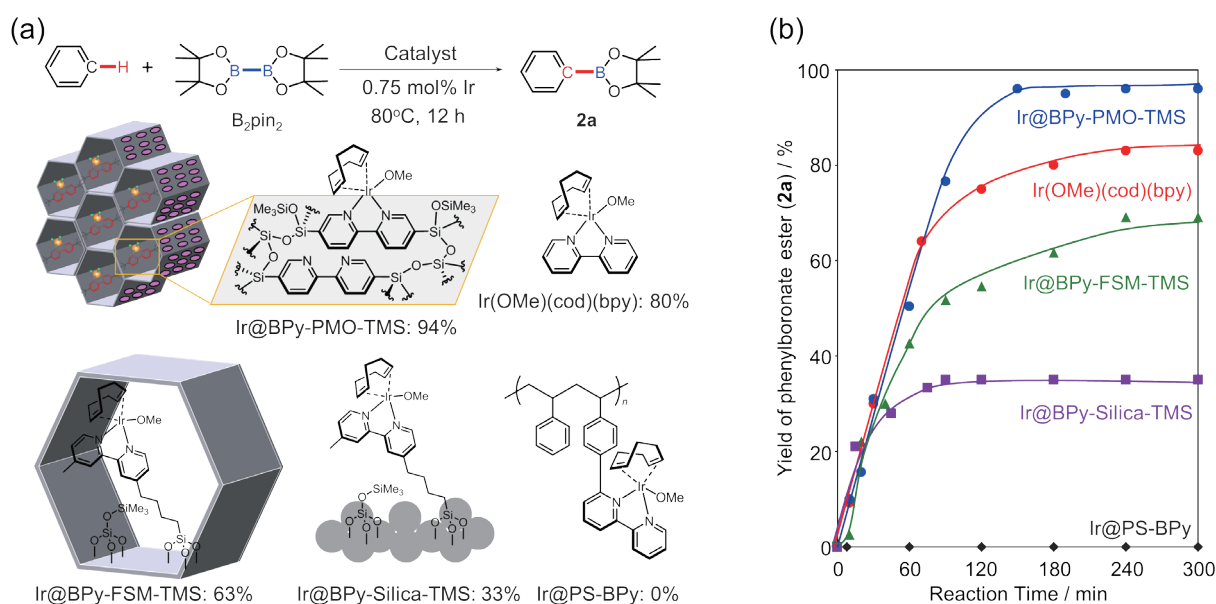
Fig. 4   (a) Schematic illustration and (b) reaction kinetic curves of direct C-H borylation of benzene with B_2pin_2 catalyzed by Ir@BPy-PMO-TMS, Ir(OMe)(cod)(bpy), Ir@BPy-FSM-TMS, Ir@BPy-Silica-TMS, and Ir@PS-BPy.

Although electron-rich benzenes bearing Me and OMe groups showed low reactivity under dilute conditions (Table 1, entries 3 and 5), these reactions efficiently proceeded under neat conditions to give the corresponding arylboronate esters **2d-e** in yields of 86-92% (Table 1, entries 4 and 6). For mono-substituted benzenes, the products were obtained as a mixture of regioisomers, where the *m*-isomer was preferentially obtained compared to the *p*-isomer, and the *o*-isomer did not form due to steric hindrance. For 1,2- and 1,3-substituted benzenes, the products **2f-i** were obtained as single regioisomers due to the steric hindrance of two substituents on the benzene ring (Table 1, entries 7-10). A wide variety of substituted heteroarenes including thiophene, furan, benzo[*b*]thiophene, benzofuran, indole and pyridine were also transformed into the corresponding heteroarylboronate esters **2j-o** in high yields of 90-93% (Table 1, entries 11-16). Thiophene, benzo[*b*]thiophene, and indole were exclusively borylated at α-positions

to the heteroatom owing to the high acidity. Furan and benzofuran rings were selectively borylated at the 2-position with the formation of the borylated product. 2,6-Disubstituted pyridine was exclusively borylated at the 4-position due to the substituents blocking the 2,6-positions.

Ir@BPy-PMO-TMS showed excellent catalytic activity for multiple C-H borylation of thiophene derivatives (**Table 2**). By using three equivalents of HBpin relative to thiophene and the ladder-type thiophene derivatives, α-positions of thiophene, 2,2'-bithiophene, and 2,2':5',2''-terthiophene were diborylated quantitatively to give products **3a-c** (Table 2, entries 1-3). Thiophene-fused benzene and thiophene derivatives such as benzo[1,2-*b*:4,5-*b*']dithiophene, thieno[3,2-*b*]thiophene, and dithieno[3,2-*b*:2',3'-*d*]thiophene were also transformed into diborylated products **3d-g** in high yields of 89-99% (Table 2, entries 4-7). The multiple C-H borylation can be utilized for the

Table 1 Direct C-H borylation of arenes and heteroarenes with HBpin catalyzed by Ir@BPy-PMO-TMS[a].

Entry	Arylboronate	Yield (%)[b]	Entry	Arylboronate	Yield (%)[b]	Entry	Arylboronate	Yield (%)[b]
1	**2b**	86[d]	8	**2g**	95	12	**2k**	93[h]
2	**2c**	91[e]	9	**2h**	94	13	**2l**	90
3	**2d**	23				14	**2m**	92[i]
4[c]		92[f]	10	**2i**	91	15	**2n**	93
5	**2e**	17						
6[c]		86[g]	11	**2j**	92	16	**2o**	92
7[c]	**2f**	68						

[a] The reactions were conducted with arenes or heteroarenes bearing functional groups (FG) (2 equiv.), HBpin (1 equiv.), and Ir@BPy-PMO-TMS (0.75 mol% Ir) in cyclohexane. [b] Isolated yields based on HBpin. [c] The reactions were carried out under neat conditions. [d] *m* : *p* = 53 : 47. [e] *m* : *p* = 69 : 31. [f] *m* : *p* = 60 : 40. [g] *m* : *p* = 51 : 49. [h] 2-isomer : 3-isomer = 86 : 14. [i] 2-isomer : 3-isomer = 80 : 20.

efficient synthesis of hole-transporting triarylamine (**Fig. 5**). After the multiple C-H borylation of tris[4-(2-thienyl)phenyl]amine, the obtained borylated product was further reacted with bromobenzene by Suzuki-Miyaura coupling to give the desired hole-transporting triarylamine (**4**) in 90% yield over two steps. The overall yield was higher than that from the conventional approach using a Grignard coupling

reaction (9%),[23] indicating multi-borylated thiophene derivatives are useful building blocks in the synthesis of functional organic materials.

3. 2 Epoxidation of Olefins

High valent dichlorodioxomolybdenum (VI) complexes such as $[MoO_2Cl_2(L)_n]$ (L: neutral ligand) are efficient

Table 2   Multiple C-H borylation of thiophene derivatives with HBpin catalyzed by Ir@BPy-PMO-TMS[a].

| Entry	Heteroarylboronate	Yield (%)[b]	Entry	Heteroarylboronate	Yield (%)[b]
1	**3a**	99	5	**3e**	95
2	**3b**	99	6	**3f**	99
3	**3c**	99	7	**3g**	89
4	**3d**	99			

[a] All reactions were conducted with thiophene derivatives (1 equiv.) and HBpin (3.0 equiv.) in the presence of Ir@BPy-PMO-TMS (1.1 mol% Ir per C–H bond in thiophene derivatives). [b] Isolated yields based on thiophene derivatives.
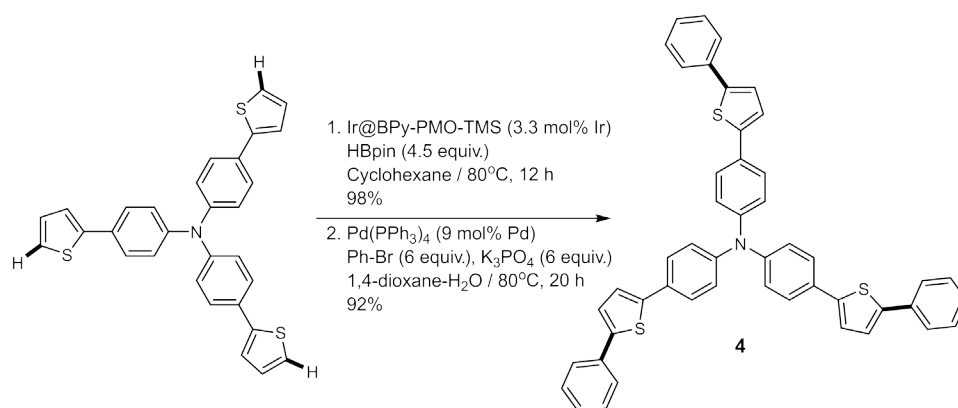
Fig. 5   Synthesis of hole-transporting triarylamine derivative **4** by multiple direct C-H borylation of tris[4-(2-thienyl)phenyl]amine followed by Suzuki-Miyaura coupling reaction.

and low-cost homogeneous catalysts for various organic reactions such as epoxidation, acylation, hydrosilylation, reduction, and oxidation.[24] Among them, $MoO_2Cl_2(bpy)$ shows an attractive catalytic activity for epoxidation of olefins with oxidants such as *tert*-butyl hydroperoxide (TBHP). Heterogenization of $MoO_2Cl_2(bpy)$ has been attempted in order to recover and reuse the catalysts. Immobilization of Mo complexes onto bipyridine-grafted mesoporous silica and bipyridine-based metal organic frameworks (BPy-MOF) has been reported.[25,26] Unfortunately, these conventional supports and immobilization approaches reduce the intrinsic catalytic activity of $MoO_2Cl_2(bpy)$.

Recently, we reported the successful immobilization of a high valent Mo(VI)-bipyridine complex by using BPy-PMO-TMS.[18] The MoO_2Cl_2 precursor was reacted with BPy-PMO-TMS, which resulted in direct formation of the Mo(VI)-bipyridine complex on the pore surface along with elimination of one chloride ligand (denoted as Mo@BPy-PMO-TMS). The loading amounts of the Mo complex could be controlled by varying the concentration of the MoO_2Cl_2 precursor in the reaction solution. The maximum loading amount of the Mo complex was 0.72 mmol g^{-1}, which means 37% of surface bipyridine ligands (BPy_{surf}) were coordinated with the Mo complex. **Figure 6** shows
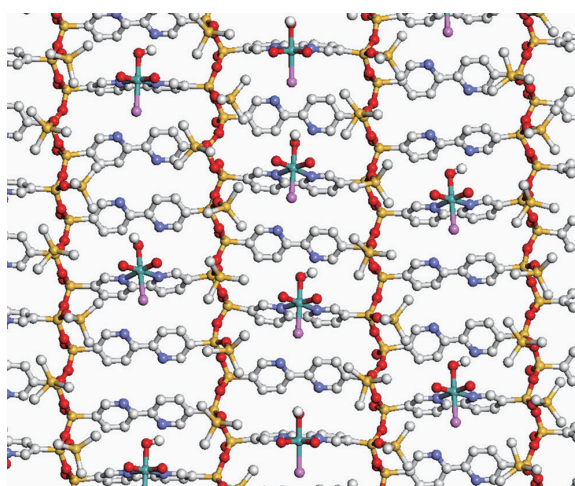
**Fig. 6** CG image of pore surface of Mo@BPy-PMO-TMS with Mo/BPy molar ratio of approximately 23% (Mo/BPy$_{surface}$ = approximately 35%). Mo: sky blue; Cl: pink; O: red; Si: orange; C: light gray; N: purple; H: omitted except for hydrogen atoms of OH ligands in Mo complexes.

a CG image of the pore surface of Mo@BPy-PMO-TMS with a Mo/BPy$_{surf}$ molar ratio of 35%, showing that BPy-PMO-TMS enables high-density immobilization of a Mo complex on the pore surface.

FT-IR and Raman spectra of Mo@BPy-PMO-TMS showed characteristic bands attributed to Mo = O stretching, where these bands were blue-shifted compared with those of the homogeneous $MoO_2Cl_2(bpy)$. This indicates that the Mo center of Mo@BPy-PMO-TMS is electron-deficient, possibly due to the direct attachment of two silicon atoms to the bipyridine ligand. The local structure of the immobilized Mo complex was investigated by XAFS measurements. The XANES spectrum of Mo@BPy-PMO-TMS showed a characteristic shoulder at 20004 eV, which is ascribed to high valent Mo(VI) species. The EXAFS oscillation and its Fourier transform were different from those of $MoO_2Cl_2(bpy)$ due to the elimination of chloride ligand from the Mo center. The EXAFS curve fitting of Mo@BPy-PMO-TMS suggested the formation of the $MoO_2Cl(OH)(bpy)$ complex on the pore surface.

Mo@BPy-PMO-TMS exhibited catalytic activity for the epoxidation of olefins. **Figure 7** shows the reaction kinetic curves for the epoxidation of *cis*-cyclooctene with TBHP at 75°C catalyzed by Mo@BPy-PMO-TMS, $MoO_2Cl_2(bpy)$, and heterogeneous Mo(VI)-bipyridine catalysts immobilized on BPy-PMO (Mo@BPy-PMO), end-capped bipyridine-grafted mesoporous silica (Mo@BPy-FSM-TMS), and polystyrene-supported bipyridine (Mo@PS-BPy). The use of Mo@BPy-PMO-TMS gave the desired epoxide (**5a**) in 67% yield after 8 h with TOF of 382 h^{-1} (initial 30 min), while homogeneous $MoO_2Cl_2(bpy)$ showed greater activity with a product yield of 90% and TOF of 881 h^{-1} under the same conditions. In contrast, Mo@BPy-FSM-TMS and Mo@PS-BPy showed low product yields of 48% and 22%, and TOFs of 141 h^{-1} and 96.1 h^{-1}, respectively. This may be attributed to the undesired interactions between the Mo center and support surface during the reaction. Mo@BPy-PMO without trimethylsilylation showed the lowest activity with a product yield of 12% and TOF of 43 h^{-1}. This result suggests that surface silanol groups interact with oxidant (TBHP) and product (epoxide) due to their hydrophilic nature, resulting in limited diffusion of these oxygenated compounds in the mesochannels. Trimethylsilylation is effective in improving the hydrophobicity of the pore surface,
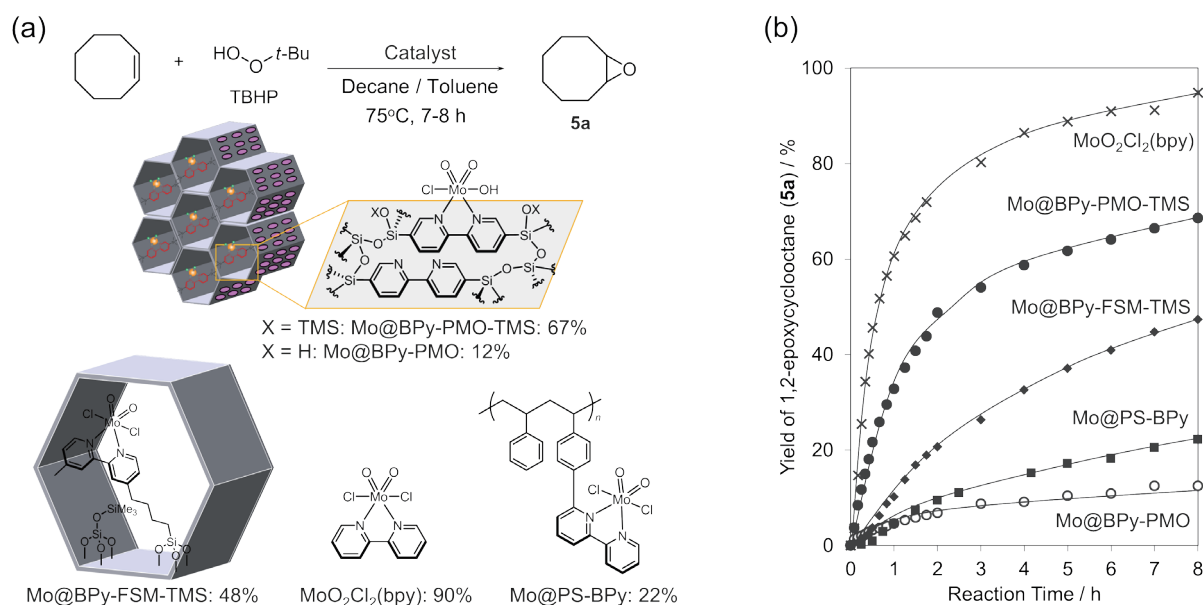
Fig. 7 (a) Schematic illustration and (b) reaction kinetic curves of epoxidation of *cis*-cyclooctene with TBHP catalyzed by Mo@BPy-PMO-TMS, Mo@BPy-PMO, MoO$_2$Cl$_2$(bpy), Mo@BPy-FSM-TMS, and Mo@PS-BPy.

which results in high product yield with high TOF for epoxidation of olefins with TBHP.

The catalytic performances of Mo@BPy-PMO-TMS and Mo@PS-BPy were further investigated by changing the loading amounts of the Mo complex on the support surface (**Fig. 8**). Interestingly, four different Mo loadings of Mo@BPy-PMO-TMS showed nearly constant TOF values of 300–400 h^{-1}. This means that immobilized Mo complexes act as a single-site catalyst for the epoxidation even with a high density of Mo complex on the pore surface. For comparison, the effect of Mo loading amounts of Mo@PS-BPy was also examined. The TOF values for Mo@PS-BPy decreased by increasing the loading amounts of the Mo complex, meaning that all of the immobilized Mo complex did not catalyze the reaction. These results indicate that well-defined and regularly arranged bipyridine groups of BPy-PMO-TMS are an attractive solid support to immobilize large amounts of Mo complex without loss of activity. From a practical viewpoint, high loading capacity of the active site is important because the same reaction outcomes can be obtained by using a small amount of catalyst, such that the reactor size can be minimized. This is also an attractive feature for the design of flow-column reactor systems because the space of the reaction bed is limited.
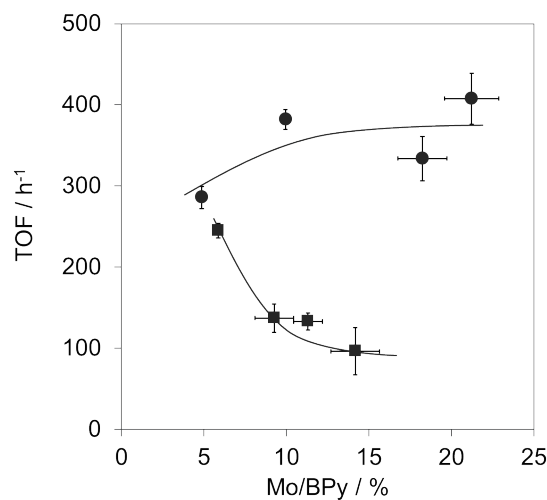
Fig. 8 Relationship between TOF value and Mo/BPy ratio of Mo@BPy-PMO-TMS (●) and Mo@PS-BPy (■). Immobilized Mo amounts were determined by ICP analysis.

The catalytic performance of Mo@BPy-PMO-TMS was significantly improved under anhydrous conditions. When the epoxidation of *cis*-cyclooctene with TBHP was carried out under anhydrous conditions, the maximum TOF of Mo@BPy-PMO-TMS reached 5200 h^{-1} under neat conditions, which is

significantly higher than that of the previously reported mesoporous silica-based Mo(VI)-bipyridine catalyst (16 h^{-1}).[(25)] Product yield and TOF were also improved by the solvent effect. The use of 1,2-dichloroethane was found to be preferable in terms of product yield and TOF. Mo@BPy-PMO-TMS showed good reusability for at least three times in the epoxidation of cis-cyclooctene with TBHP in 1,2-dichloroethane under anhydrous conditions.

Mo@BPy-PMO-TMS showed excellent catalysis for the epoxidation of a variety of olefins including aliphatic and aromatic groups under optimized conditions (**Table 3**). The epoxidation of cyclic olefins such as cis-cyclooctene and cyclohexene occurred quantitatively within 3 h to give the corresponding epoxides **5a-b** (Table 3, entries 1-2). Internal aliphatic olefins such as cis-2-octene and trans-2-octene were transformed into the corresponding epoxides **5c-d** almost quantitatively (Table 3, entries 3-4). In

contrast, a terminal aliphatic olefin such as 1-octene showed moderate activity for epoxidation to afford 1,2-epoxyoctane (**5e**) in 61% yield (Table 3, entry 5). When limonene was used as a substrate, the endocyclic double bond was regioselectively epoxidized to give limonene oxide (**5f**) in 87% yield (Table 3, entry 6). An aromatic olefin such as styrene was also oxidized to afford styrene oxide (**5g**) in 78% yield, although unidentified side products were produced (Table 3, entry 7). When the epoxidation of cis-stilbene and trans-stilbene was carried out, the cis-isomer was perfectly oxidized after 24 h to transform into cis-stilbene oxide (**5h**) in 96% yield (Table 3, entry 8). In contrast, trans-stilbene oxide (**5i**) was obtained in slightly lowered yield of 82% under identical conditions, possibly due to steric hindrance from the diphenyl groups of the substrate (Table 3, entry 9). The catalytic performance of Mo@BPy-PMO-TMS was comparable to that of homogeneous MoO$_2$Cl$_2$(bpy)

Table 3 Epoxidation of olefins with TBHP catalyzed by Mo@BPy-PMO-TMS[a].

Entry	Epoxide	Yield (%)[b]	Entry	Epoxide	Yield (%)[b]
1	**5a**	100 (100)	6[c]	**5f**	87 (69)
2	**5b**	100 (100)	7	**5g**	78 (48)
3	**5c**	100 (100)	8	**5h**	96 (98)
4	**5d**	99 (99)	9	**5i**	82 (84)
5	**5e**	61 (71)			

[a] All reactions were conducted with olefins (2.5 mmol), TBHP (3.75 mmol), and dry mesitylene or dry 1,4-dioxane (1.0 mmol, internal standard) in the presence of Mo@BPy-PMO-TMS (35 mg, 10 μmol Mo) or MoO$_2$Cl$_2$(bpy) (3.6 mg, 10 μmol Mo) in dry 1,2-dichloroethane (4.3 mL) at 75°C. [b] ^{1}H NMR yields based on internal standard. ^{1}H NMR yields for homogeneous catalytic system using MoO$_2$Cl$_2$(bpy) are given in parentheses. [c] The reaction was carried out at 50°C.

catalyst, indicating Mo@BPy-PMO-TMS is a good heterogeneous catalyst for epoxidation of a variety of olefins.

4. Conclusions

In this report, we describe the synthesis of BPy-PMO and recent advances in the development of well-defined heterogeneous metal complex catalysts based on BPy-PMO as a solid support. BPy-PMO is an ideal platform to generate a well-defined organometallic site on the pore surface without change in the local structure of the original homogeneous metal complex catalyst. Since the metal complexes were strongly immobilized into the robust pore framework without aggregation and undesired interactions, BPy-PMO-based metal complex catalysts showed not only high catalytic activity but also reusability for various organic transformations. We demonstrated the high catalytic performance of the BPy-PMO-based Ir complex catalyst for direct C-H borylation of arenes and heteroarenes with bis(pinacolate)diboron or pinacolborane, and BPy-PMO-based Mo complex catalyst for epoxidation of olefins with *tert*-butyl hydroperoxide. By using a crystal-like pore wall of BPy-PMO, unique reaction fields can be constructed in the mesochannels that cannot be achieved in homogeneous solution systems. For example, co-immobilization of two kinds of metal complexes on the same pore surface allowed us to develop the rational design of efficient photocatalytic reaction systems.[27,28] Use of BPy-PMO will open new immobilization approaches to advance chemistry on metal complex catalyzed organic reactions from solution systems to solid-state systems aimed for industrial processes.

Acknowledgements

References

(1) Cornils, B. and Herrmann, W. A., *Applied Homogeneous Catalysis with Organometallic Compounds* (1996), pp. 27-572, Wiley-VCH.

(2) Li, C., *Catal. Rev.*, Vol. 46, No. 3-4 (2004), pp. 419-492.

(3) Inagaki, S., Guan, S., Fukushima, Y., Ohsuna, T. and Terasaki, O., *J. Am. Chem. Soc.*, Vol. 121, No. 41 (1999), pp. 9611-9614.

(4) Asefa, T., MacLachlan, M. J., Coombs, N. and Ozin, G. A., *Nature*, Vol. 402, No. 6764 (1999), pp. 867-871.

(5) Melde, B. J., Holland, B. T., Blanford, C. F. and Stein, A., *Chem. Mater.*, Vol. 11, No. 11 (1999), pp. 3302-3308.

(6) Waki, M., Mizoshita, N., Ohsuna, T., Tani, T. and Inagaki, S., *Chem. Commun.*, Vol. 46, No. 43 (2010), pp. 8163-8165.

(7) Waki, M., Mizoshita, N., Tani, T. and Inagaki, S., *Angew. Chem. Int. Ed.*, Vol. 50, No. 49 (2011), pp. 11667-11671.

(8) Waki, M., Maegawa, Y., Hara, K., Goto, Y., Shirai, S., Yamada, Y., Mizoshita, N., Tani, T., Chun, W.-J., Muratsugu, S., Tada, M., Fukuoka, A. and Inagaki, S., *J. Am. Chem. Soc.*, Vol. 136, No. 10 (2014), pp. 4003-4011.

(9) Waki, M., Maegawa, Y., Mizoshita, N., Tani, T. and Inagaki, S., *R&D Review of Toyota CRDL*, Vol. 47, No. 1 (2016), pp. 57-66.

(10) Ishito, N., Kobayashi, H., Nakajima, K., Maegawa, Y., Inagaki, S., Hara, K. and Fukuoka, A., *Chem. -Eur. J.*, Vol. 21, No. 44 (2015), pp. 15564-15569.

(11) Maegawa, Y. and Inagaki, S., *Dalton Trans.*, Vol. 44, No. 29 (2015), pp. 13007-13016.

(12) Liu, X., Maegawa, Y., Goto, Y., Hara, K. and Inagaki, S., *Angew. Chem., Int. Ed.*, Vol. 55, No. 28 (2016), pp. 7943-7947.

(13) Yoshida, M., Saito, K., Matsukawa, H., Yanagida, S., Ebina, M., Maegawa, Y., Inagaki, S., Kobayashi, A. and Kato, M., *J. Photochem. Photobiol., A Chem.*, Vol. 358 (2018), pp. 334-344.

(14) Naganawa, Y., Maegawa, Y., Guo, H., Gholap, S. S., Tanaka, S., Sato, K., Inagaki, S. and Nakajima, Y., *Dalton Trans.*, Vol. 48, No. 17 (2019), pp. 5534-5540.

(15) Matsui, K., Maegawa, Y., Waki, M., Inagaki, S. and Yamamoto, Y., *Catal. Sci. Technol.*, Vol. 8, No. 2 (2018), pp. 534-539.

(16) Ishito, N., Nakajima, K., Maegawa, Y., Inagaki, S. and Fukuoka, A., *Catal. Today*, Vol. 298 (2017), pp. 258-262.

(17) Wang, X., Thiel, I., Fedorov, A., Copéret, C., Mougel, V. and Fontecave, M., *Chem. Sci.*, Vol. 8, No. 12 (2017), pp. 8204-8213.

(18) Ishikawa, S., Maegawa, Y., Waki, M. and Inagaki, S., *ACS Catal.*, Vol. 8, No. 5 (2018), pp. 4160-4169.

(19) Ishikawa, S., Maegawa, Y., Waki, M. and Inagaki, S., *Appl. Catal., A*, Vol. 575 (2019), pp. 87-92.

(20) Mkhalid, I. A. I., Barnard, J. H., Marder, T. B.,
     Murphy, J. M. and Hartwig, J. F., *Chem. Rev.*, Vol. 110,
     No. 2 (2010), pp. 890-931.

(21) Hall, D. G., *Boronic Acids: Preparation and
     Applications in Organic Synthesis and Medicine*
     (2005), pp. 1-99, Wiley-VCH Verlag.

(22) Ishiyama, T., Takagi, J., Ishida, K., Miyaura, N.,
     Anastasi, N. R. and Hartwig, J. F., *J. Am. Chem. Soc.*,
     Vol. 124, No. 3 (2002), pp. 390-391.

(23) Kageyama, H., Ohishi, H., Tanaka, M., Ohmori, T.
     and Shirota, Y., *Adv. Funct. Mater.*, Vol. 19, No. 24
     (2009), pp. 3948-3955.

(24) Jeyakumar, K. and Chand, D. K., *J. Chem. Sci.*,
     Vol. 121, No. 2 (2009), pp. 111-123.

(25) Nunes, C. D., Valente, A. A., Pillinger, M., Fernandes,
     A. C., Romão, C. C., Rocha, J. and Gonçalves, I. S., *J.
     Mater. Chem.*, Vol. 12, No. 6 (2002), pp. 1735-1742.

(26) Leus, K., Liu, Y.-Y., Meledina, M., Turner, S.,
     Van Tendeloo, G. and Van der Voort, P., *J. Catal.*,
     Vol. 316 (2014), pp. 201-209.

(27) Kuramochi, Y., Sekine, M., Kitamura, K.,
     Maegawa, Y., Goto, Y., Shirai, S., Inagaki, S. and
     Ishida, H., *Chem. - Eur. J.*, Vol. 23, No. 43 (2017),
     pp. 10301-10309.

(28) Waki, M., Yamanaka, K., Shirai, S., Maegawa, Y.,
     Goto, Y., Yamada, Y. and Inagaki, S., *Chem. Eur. J.*,
     Vol. 24, No. 15 (2018), pp. 3846-3853.

Yoshifumi Maegawa
  Research Fields:
    - Organic Synthesis for Functional
      Organosilane Precursors
    - Synthesis and Application of Periodic
      Mesoporous Organosilicas
  Academic Societies:
    - The Chemical Society of Japan
    - The Society of Synthetic Organic Chemistry, Japan